

# Interphase Microtubules Determine the Initial Alignment of the Mitotic Spindle

Sven K. Vogel,<sup>1,2</sup> Isabel Raabe,<sup>1,2</sup> Aygül Dereli,<sup>1</sup> Nicola Maghelli,<sup>1</sup> and Iva Tolić-Nørrelykke<sup>1,\*</sup>

<sup>1</sup>Max Planck Institute of Molecular Cell Biology and Genetics  
Dresden 01307  
Germany

## Summary

In the fission yeast *Schizosaccharomyces pombe*, interphase microtubules (MTs) position the nucleus [1, 2], which in turn positions the cell-division plane [1, 3]. It is unclear how the spindle orients, with respect to the predetermined division plane, to ensure that the chromosomes are segregated across this plane. It has been proposed that, during prometaphase, the astral MT interaction with the cell cortex aligns the spindle with the cell axis [4] and also participates in a spindle orientation checkpoint (SOC), which delays entry into anaphase as long as the spindle is misaligned [5–7]. Here, we trace the position of the spindle throughout mitosis in a single-cell assay. We find no evidence for the SOC. We show that the spindle is remarkably well aligned with the cell longitudinal axis at the onset of mitosis, by growing along the axis of the adjacent interphase MT. Misalignment of nascent spindles can give rise to anucleate cells when spindle elongation is impaired. We propose a new role for interphase microtubules: through interaction with the spindle pole body, interphase microtubules determine the initial alignment of the spindle in the subsequent cell division.

## Results and Discussion

### Spindles Are Well Aligned with the Cell Longitudinal Axis at the Beginning of Mitosis

We measured the position of the spindle pole bodies (SPBs, centrosome equivalents in yeasts), before and during mitosis, with high temporal resolution (5 s) and spatial precision (40 nm/pixel) in wild-type cells expressing the Sid4-GFP fusion protein as an SPB marker (Figures 1A–1C and Figure S1 in the Supplemental Data available online). We measured the spindle length and the angle  $\alpha$  between the spindle axis and the cell longitudinal axis (inset in Figure 1B). When mitosis started, newly formed spindles of  $\sim 0.5 \mu\text{m}$  in length were well aligned along the cell longitudinal axis, with  $\alpha \sim 10^\circ$  (Figures 1B–1D, 1H; Table 1).

### Initial Spindle Alignment Is Determined by the Alignment of the Interphase MTs Attached to the SPB

In *S. pombe*, interphase MTs lie approximately parallel to the cell axis ( $\alpha = 5.3^\circ \pm 0.8^\circ$ , mean  $\pm$  SEM,  $n = 30$ ,

Table S5). The SPB duplicates long before mitosis [8, 9]; the two parts are connected and attached to the outside of the nuclear envelope and to interphase MTs [8]. At the onset of mitosis, the interphase MTs disassemble, while the two SPBs begin to move apart by growth and sliding of interpolar MTs [10]. We noticed that the SPBs separated apparently along the axis of the interphase MT to which they were attached (Figure 1D). This observation led us to hypothesize that interphase MTs guide the alignment of the duplicated SPB prior to mitosis, which in turn defines the initial alignment of the mitotic spindle parallel to the cell longitudinal axis. This hypothesis predicts that impaired interphase MTs, or attachment of the MTs to the SPB, should lead to misalignment of newly formed spindles.

In order to examine the role of SPB-MT attachment in initial spindle alignment, we used a mutant lacking Mto1p (also known as Mod20p and Mbo1p), a centrosome-related protein that is required for the recruitment of the  $\gamma$ -tubulin complex to cytoplasmic MT-organizing centers, including the cytoplasmic face of the SPB [11, 12]. *mto1* $\Delta$  cells thus are defective in MT nucleation and in the attachment of interphase MTs to the SPB: interphase MTs are absent in 20% of cells, and the SPB is disconnected from MTs in 71% of cells with MTs [13]. We found that *mto1* $\Delta$  spindles were formed at a significantly larger angle than wild-type spindles (Figure 1H, Table S5). We conclude that defects in interphase MT attachment to the SPB lead to initial spindle misalignment.

Next we hypothesized that cells with normal MT nucleation and a normal SPB-MT attachment may form misaligned spindles if the dynamics of interphase MTs is impaired. If the interphase MTs are, on average, not much longer than the cell width, they may be less constrained by the cell shape and hence more misaligned than long MTs. As a consequence, the spindles formed in the following cell division may be misaligned. This hypothesis was tested with a *mal3* $\Delta$  mutant: Mal3p is an EB1 homolog, which associates with MTs and suppresses MT catastrophe [14, 15], and thus, *mal3* $\Delta$  cells have short interphase MTs [14, 15]. In comparison with wild-type, we found that the newly formed *mal3* $\Delta$  spindles were significantly more misaligned, often clearly following the axis of the interphase MT to which they were attached (Figures 1E, 1F, and 1H, Figure S2, Tables S3 and S5). The *mal3* $\Delta$  interphase MTs were, on average, misaligned to a similar extent as the *mal3* $\Delta$  spindles ( $p = 0.47$ , Table S5). These results are consistent with the above hypothesis that the axis of a nascent spindle follows the axis of the interphase MT attached to the SPB.

To further test the role of MTs in spindle alignment, we depolymerized interphase MTs by using MBC (see Supplemental Data). The cells that entered mitosis in the constant presence of MBC displayed highly misaligned spindles (Figure 1H, Table S5). To exclude the possibility that this misalignment results from the effect of MBC on spindle MTs, a control experiment was performed where MBC was washed out after 45 min of treatment and the

\*Correspondence: tolic@mpi-cbg.de

<sup>2</sup>These authors contributed equally to this work.

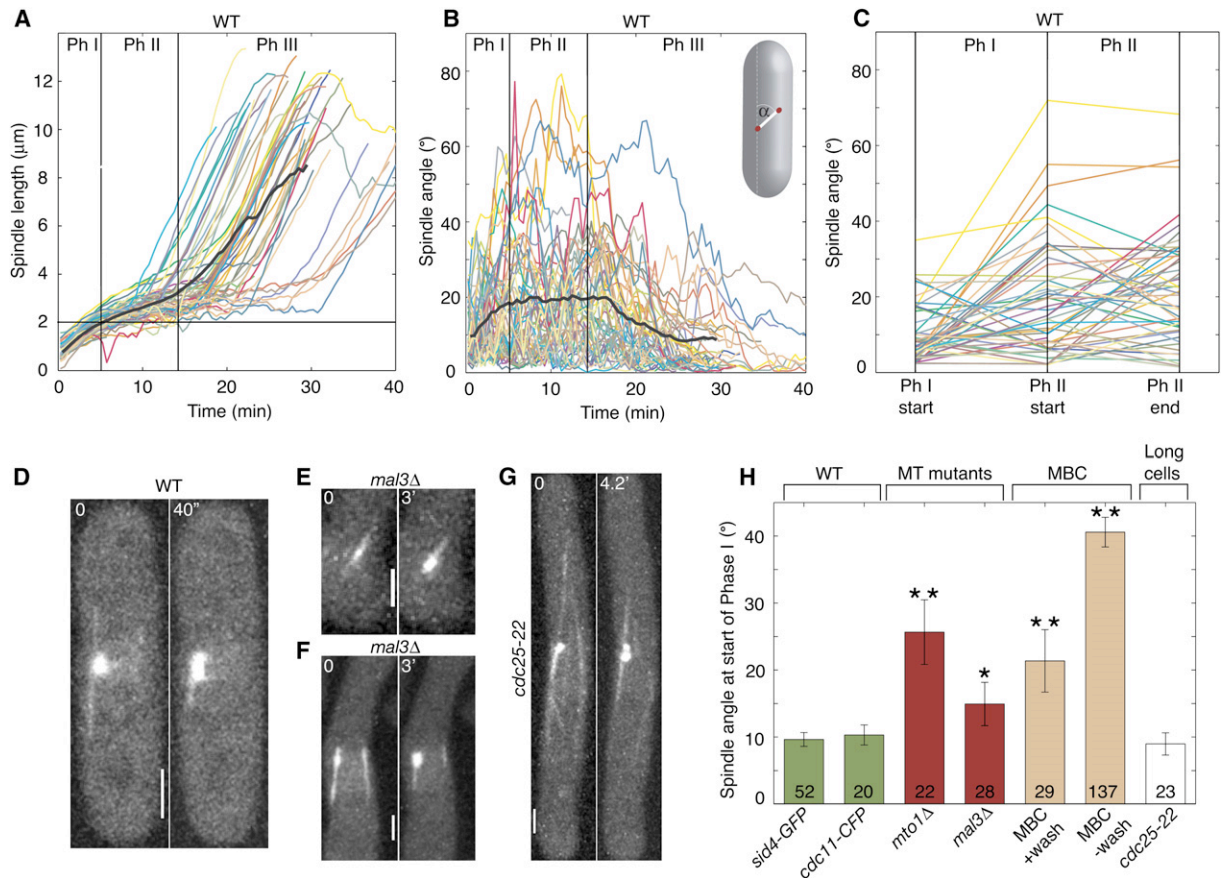


**Figure 1. Initial Spindle Alignment Follows the Alignment of the Interphase Microtubules Attached to the Spindle Pole Body**

(A) Spindle length as a function of time for a set of 52 wild-type cells expressing Sid4-GFP as an SPB marker. Each cell is represented by a different color; the black line shows the mean. Spindle elongation in *S. pombe* occurs in three phases [26]. During Phase I (prophase or spindle formation), the spindles elongate from 0 to  $\sim 2 \mu\text{m}$  in  $\sim 5$  min. In Phase II (prometaphase or the phase of interaction between chromosomes and the spindle), the spindles spend  $\sim 10$  min at a length of 2–3  $\mu\text{m}$ . In Phase III (anaphase B or the separation of chromosomes), the spindles grow to a length of  $\sim 12 \mu\text{m}$  in  $\sim 15$  min. See [Movie S1](#).

(B) Spindle angle ( $\alpha$ ) as a function of time for the same set of cells with the same color code as in (A).  $\alpha$  is defined as the absolute angle (deviation angle) between the spindle axis and the cell longitudinal axis in 2 dimensions (see inset), with possible values from  $0^\circ$  to  $90^\circ$ . The mean  $\alpha$  (black line) is  $\sim 10^\circ$  at the onset of mitosis, it increases to  $\sim 20^\circ$  during Phase I, and it remains steady during Phase II. Note that during Phases I and II, the spindle is shorter than the cell width (cell width  $\sim 3 \mu\text{m}$ , cell length  $\sim 12 \mu\text{m}$ ), implying that the spindle is, in principle, free to assume any angle. The alignment of the spindles improves again during Phase III, as the spindles elongate beyond the cell width and are, therefore, constrained to smaller angles by the cell geometry.

(C) Spindle angle ( $\alpha$ ) at the beginning of Phase I, at the beginning of Phase II, and at the end of Phase II for each cell from the set shown in (A) and (B).  $\alpha$  increases during Phase I in 73% of the cells and decreases in the remaining 27% ( $n = 51$ ). During Phase II,  $\alpha$  increases in 54% of the cells and decreases in the remaining 46% ( $n = 48$ ).

(D) Selected maximum-intensity projections from a time-lapse sequence of a cell expressing GFP-tubulin, as it enters mitosis ([Movie S2](#)). Note that at 40 s, the spindle (bright bar) forms parallel to the cell longitudinal axis, apparently following the axis of the adjacent interphase MT (thin line).

(E) A *mal3Δ* cell expressing GFP-tubulin, before (left) and after (right) SPB separation. The nascent spindle is misaligned ( $\alpha = 40^\circ$ ), following the axis of the adjacent interphase MT. See [Movie S3](#).

(F) In a *mal3Δ* cell in which the SPB-attached interphase MT is well aligned, the nascent spindle is also well aligned ( $\alpha = 5^\circ$ ).

(G) A *cdc25-22* cell expressing Sid4-GFP and GFP-tubulin before (left) and after (right) SPB separation. The interphase MTs are well aligned, but they do not reach the cell tips in these elongated cells. The spindle is formed well aligned, along one of the well-aligned interphase MTs. See [Movie S4](#). Scale bars in (D)–(G) represent 2  $\mu\text{m}$ .

(H) Spindle angle at the beginning of mitosis, when the spindle length is  $\sim 500$  nm. Two wild-type strains expressing either Sid4-GFP or Cdc11-CFP formed well-aligned spindles (green bars). On the contrary, the spindles of two mutants with MT-defects (*mto1Δ* and *mal3Δ*) were misaligned (red). The spindles were also misaligned in cells treated with MBC, either with or without MBC wash-out before mitosis (light brown), though the misalignment was highly significantly ( $p < 0.005$ ) larger without the wash-out than with wash-out ( $p = 4 \cdot 10^{-4}$ ). In a mutant with normal MTs, but increased cell length (*cdc25-22*), the spindles were well aligned (white). The number of cells in each group is given in the bar. Error bars indicate SEM. Asterisks: t test comparison with wild-type (*sid4-GFP*), \*, significant ( $0.005 < p < 0.05$ ); \*\*, highly significant ( $p < 0.005$ ).

cells entered mitosis in MBC-free medium. The newly forming spindles were found to be significantly more misaligned than in untreated cells, though to a smaller extent than those formed in the presence of MBC

([Figure 1H](#), [Table S5](#)). This may be a consequence of the MBC wash-out, allowing for repolymerization of interphase MTs to some extent before the next mitosis. Taken together, these data suggest that the absence

Table 1. Wild-Type Spindle Dynamics

Wild-Type Strain Expressing Sid4-GFP	Mean $\pm$ SEM	n	p
Angle at the beginning of Phase I	9.6° $\pm$ 1.0°	52	-
Angle at the beginning of Phase II	19.8° $\pm$ 2.1°	52	3 · 10 <sup>-5</sup>
Angle at the end of Phase II	22.2° $\pm$ 2.1°	48	0.19
Duration of Phase I	5.5 $\pm$ 0.3 min	52	
Duration of Phase II	12.1 $\pm$ 0.9 min	46	
Spindle length at the end of Phase II	3.0 $\pm$ 0.1 $\mu$ m	48	
Spindle elongation rate in Phase III	0.63 $\pm$ 0.02 $\mu$ m/min	48	

n, number of cells; p, p values from a paired t test of the hypothesis that the two samples of angles ( $\alpha$ ) come from distributions with equal means.  $\alpha$  at the beginning of Phase II was highly significantly different than  $\alpha$  at the beginning of Phase I ( $p = 3 \cdot 10^{-5}$ );  $\alpha$  at the end of Phase II was not significantly different than  $\alpha$  at the beginning of Phase II ( $p = 0.19$ ).

of interphase MTs leads to misalignment of nascent spindles.

To assess the role of the interaction between the interphase MTs and the cell tips in spindle alignment, we analyzed the temperature-sensitive *cdc25-22* mutant, which has normal MTs but a reduced MT cell tip interaction resulting from an increased cell length after cell-cycle block and release [16]. We observed well-aligned spindles and well-aligned interphase MTs in this mutant, as in wild-type (Figures 1G and 1H, Table S5). Interphase MTs of this mutant are most likely forced to be well aligned owing to their length, similar to the MTs in wild-type [17]. Our data suggest that *local* alignment of the interphase MTs at the site of their attachment to the SPB determines the alignment of the nascent spindle, whereas the interaction between the interphase MTs and the cell tip is not crucial for spindle alignment. Detachment of the SPB from interphase MTs, predominance of short misaligned interphase MTs, as well as absence of interphase MTs, lead to misalignment of nascent spindles.

### The Effect of Astral Microtubules on Spindle Rotation in Phases II and III

Astral MTs push on the SPBs in Phase III [18], but it is not clear whether they exert forces on the spindle during Phase II [4, 6]. We measured the movement of the Phase II SPB while an astral MT was emanating from it (Figures 2A and 2B, Table 2). The mean SPB movement was not significantly different from zero (Table 2), and the absolute movement of the SPB was small (Figure 2A, Table 2). These results suggest that Phase II astral MTs do not move or rotate the spindle significantly. Furthermore, rotation of the spindle, to a similar extent, was observed in the same cells during asterless time intervals in Phase II, indicating that astral MTs are not necessary for spindle rotation. We conclude that in Phase II, astral MTs, which are at this stage intranuclear [19], can exert transient forces on the SPBs, but they are neither necessary nor sufficient for spindle rotation. The mechanism of spindle rotation during Phase II awaits further investigation.

We next examined the relative importance of astral MT pushing on the SPBs and of the cell shape on spindle alignment during Phase III. We measured the number of strong pushing events (>200 nm) per cell. These events were rare (0–3 times during Phase III, Table 2). Thus, we propose that pushing of astral MTs might help to align the spindle, whereas the key to spindle alignment during Phase III is the cylindrical shape of the cell, which forces an elongating spindle to align with the cell's longitudinal axis.

### Spindle Orientation Checkpoint Does Not Operate in *S. pombe*

We asked whether spindle alignment affects progress through mitosis. A number of recent studies have suggested a spindle orientation checkpoint (SOC) in *S. pombe* [4–7, 20] (reviewed in [21, 22]), analogous to the established SOC in *Saccharomyces cerevisiae* [23]. According to the SOC idea, well-aligned spindles start anaphase on schedule, whereas misaligned spindles exhibit a metaphase delay until they become aligned. The previous evidence for existence of an SOC in *S. pombe* is based on partial depolymerization of actin [5–7] and on the *mia1* mutation that abolishes astral MTs [4]. In both cases, misaligned spindles and a Phase II delay were observed. However, it is not clear whether the Phase II delay was a consequence of spindle misalignment, or vice versa, or whether both observations were caused by another defect induced by the mutation or the drug treatment.

A direct way to test the idea of SOC is a single-cell analysis of the correlation between spindle angles and the progress through mitosis. If SOC operates, then the cells that have a misaligned spindle should exhibit a longer Phase II than the cells with aligned spindles. Surprisingly, we found no correlation between the duration of Phase II and the spindle angle in wild-type cells (Figures 2C and 2E, Figure S3).

Because very few wild-type cells have highly misaligned Phase II spindles that would merit a checkpoint intervention, we tested *mia1* $\Delta$  cells, which show misalignment more frequently [4] (Figure S2, Table S4). Yet, the duration of Phase II was not correlated with the spindle angle in *mia1* $\Delta$  cells (Figures 2D and 2E).

Furthermore, if there is an SOC, then misaligned spindles should align before the start of Phase III. We observed that the misaligned spindles became somewhat better aligned during Phase II, while the aligned spindles became slightly less aligned (Figure S3). This result is more compatible with a random change of the spindle angle than with an active mechanism that aligns the spindle during Phase II. Taken together, our data are not consistent with a checkpoint for spindle alignment per se (SOC) in fission yeast.

Why does *S. pombe*, in contrast to *S. cerevisiae*, proceed with mitosis without checking the spindle alignment? The answer probably lies in the different geometries of the two yeasts. The cylindrical shape of *S. pombe* cells facilitates mitosis: the cell shape forces an elongating spindle to align with the cell longitudinal axis, which results in a correct separation of the genetic material toward the tips of the future daughter cells. The budded shape of *S. cerevisiae*, on the other hand, provides a difficulty for mitosis: one pole of the spindle,

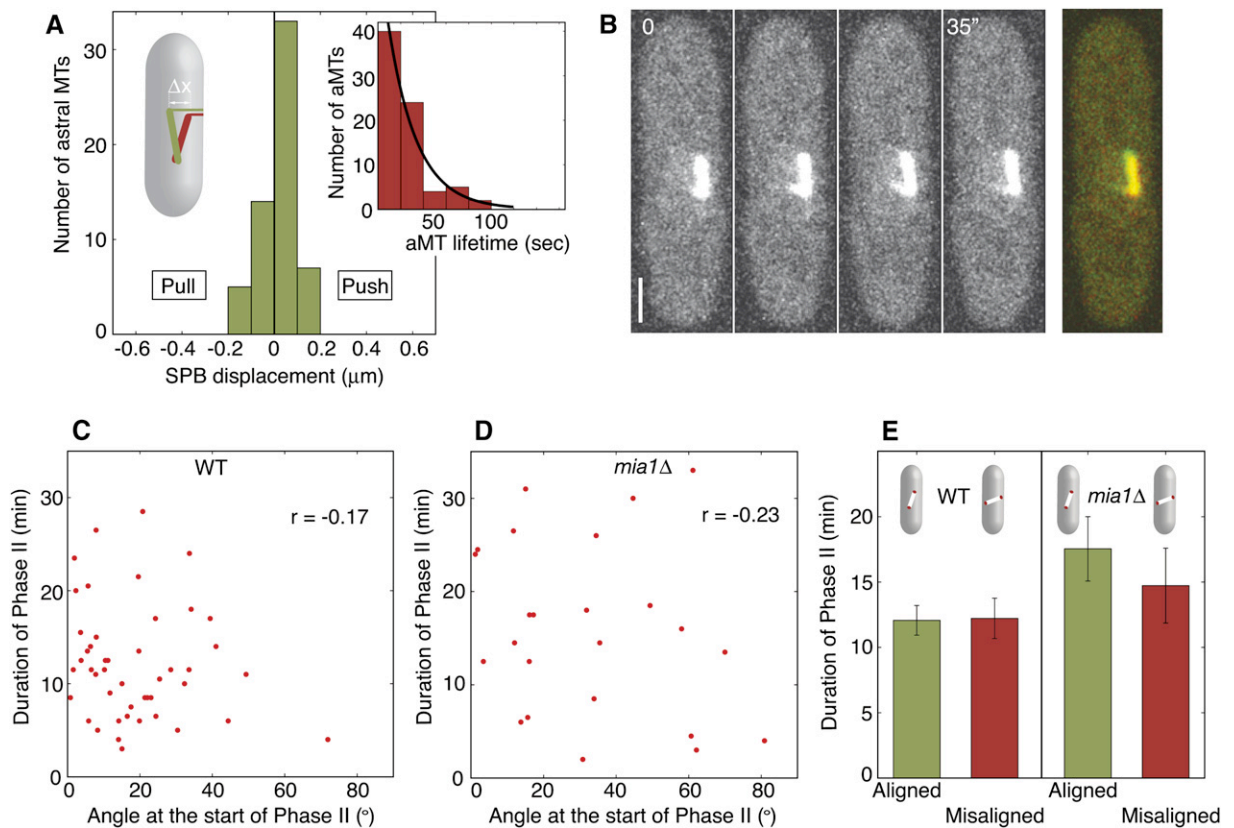


Figure 2. Spindle Orientation Checkpoint Does Not Operate in *S. pombe*

(A) Astral MTs do not displace the SPB significantly during Phase II. A histogram (green) of the SPB displacement (see the drawing) during the lifetime of a single astral MT emanating from the SPB. Positive displacements are consistent with astral MT pushing on the SPB, negative displacements with pulling. The mean SPB movement was not significantly different from zero. The absolute movement of the SPB was small, below 200 nm, which corresponds to a spindle rotation of  $<6^\circ$ . Inset histogram (red): astral MT (aMT) lifetime in Phase II, measured as the time interval between the image where an astral MT appeared and the image where it disappeared. Assuming a constant probability of catastrophe (a Poisson process), which would yield an exponential distribution of MT growth times, an exponential fit to the data is shown.

(B) Example of a Phase II astral MT that did not induce a significant rotation of the spindle. Left: a selection from the time-lapse sequence of a wild-type cell expressing GFP-tubulin (Movie S5). Right: an overlay of the first image (red) and the last image (green) to better visualize the movement of the spindle. Scale bar represents 2  $\mu\text{m}$ .

(C) Duration of Phase II in wild-type was not correlated with the spindle angle at the beginning of Phase II ( $n = 46$ ,  $r = -0.17$ ,  $p = 0.27$ ).

(D) Duration of Phase II in *mia1* $\Delta$  was not correlated with the spindle angle at the beginning of Phase II ( $n = 24$ ,  $r = -0.23$ ,  $p = 0.28$ ).

(E) Misaligned wild-type spindles ( $\alpha > 20^\circ$  at the beginning of Phase II) did not spend a longer time in Phase II than the aligned wild-type spindles ( $\alpha < 20^\circ$ ):  $p = 0.94$ ,  $n = 28$  aligned and 18 misaligned spindles. Misaligned *mia1* $\Delta$  spindles did not spend a longer time in Phase II than the aligned *mia1* $\Delta$  spindles:  $p = 0.47$ ,  $n = 11$  aligned and 13 misaligned spindles. Error bars indicate SEM.

which is formed in the mother cell, has to pass through the narrow neck into the bud. Thus, a checkpoint mechanism for the spindle position and alignment is necessary in budding yeast to ensure that the bud actually receives a nucleus.

#### Initial Misalignment of the Spindle Can Lead to Unequal Nuclear Segregation when Spindle Elongation Is Slow

If the degree of early spindle alignment does not affect progression through mitosis in normal growth conditions, then what is the biological significance of spindle alignment? We hypothesized that proper spindle alignment promotes correct segregation of the two sets of chromosomes across the division plane. Spindle alignment depends on three mechanisms: interphase MTs (1) align the spindle at the beginning of Phase I, whereas cell shape (2) and astral MTs (3) align the spindle during Phase III. In order to test the significance of the first

mechanism (interphase MTs), we perturbed the other two (cell shape and astral MTs) by treating the cells with the MT-depolymerizing agent MBC. MBC abolished the astral MTs mechanism because astral MTs were absent during Phase III in MBC-treated cells (Figure S4). The efficiency of the cell shape alignment mechanism was decreased by MBC based on the following observation: MBC treatment decreased the spindle elongation rate in Phase III without affecting the time of septum formation, the key time after which eventual mis-segregation of chromosomes cannot be corrected (Table S6). Thus, compared with untreated spindles, the MBC-treated spindles were shorter, and consequently their angle was less constrained by cell shape at the time of septum formation (Table S6).

We first treated the cells with MBC during Phase II to abolish the cell shape and astral MTs mechanism, but not the interphase MTs mechanism, and we measured the frequency of equal nuclear segregation (one SPB per

Table 2. Astral MT Behavior in Phases II and III

	Phase II	Phase III
Astral MT lifetime <sup>a</sup>	25 ± 2 s (n <sub>a</sub> = 75)	39 ± 2 s (n <sub>a</sub> = 278)
Contact time with the cell cortex <sup>b</sup>	-	28 ± 2 s (n <sub>a</sub> = 133)
p value, t test for zero SPB movement <sup>c</sup>	0.06 (n <sub>a</sub> = 59)	0.008 (n <sub>a</sub> = 57)
Astral MTs that push >200 nm <sup>d</sup>	<2% (0/59)	12% (7/57)
Maximum push on SPB <sup>e</sup>	160 nm	600 nm

Astral MT Number per Cell

Total number	4.4 ± 0.7 (n <sub>c</sub> = 17)	13.1 ± 1.0 (n <sub>c</sub> = 23)
Number of aMTs that contact cell cortex	0	6.5 ± 0.7
Number of aMTs that push >200 nm	0	1.3 ± 0.8

<sup>a</sup> Astral MT (aMT) lifetime was measured as the time interval between the first and the last image where an aMT was present.

<sup>b</sup> aMTs typically did not contact the cell cortex in Phase II, whereas ~50% of the Phase III aMTs did contact the cell cortex for >5 s.

<sup>c</sup> p value from a t test of the hypothesis that the displacement data (of the SPB during the lifetime of an aMT) come from a distribution with mean zero.

<sup>d</sup> Fraction of aMTs during the lifetime of which the SPB moved by >200 nm in the direction away from this aMT, consistent with aMT pushing on the SPB.

<sup>e</sup> Maximum movement of the SPB during the lifetime of an aMT. n<sub>a</sub>, number of aMTs; n<sub>c</sub>, number of cells. Data are shown as mean ± SEM.

daughter cell; **Figures 3A and 3C**) versus unequal nuclear segregation (0 or 2 SPBs per daughter cell; **Figures 3A and 3B**). The cells treated with MBC during Phase II finished mitosis with equal nuclear segregation (n = 16 out of 16 cells).

Next, we treated the cells with MBC before mitosis to abolish all three mechanisms of spindle alignment. The initial spindle angle was random, most likely because of the absence of interphase MTs (**Figure 1H**, **Table S5**). Remarkably, 31% of the cells that went through mitosis segregated the nuclei unequally (n = 137; **Figure 3B**, **Figure S4**). Moreover, the cells with highly misaligned spindles at the beginning of mitosis (70° < α < 90°) showed unequal nuclear segregation 7.5 times more frequently than the cells with initially aligned spindles (α < 20°; **Figures 3D and 3E**). Our explanation of these results is that, even when elongating slowly, aligned spindles typically cross the septum before its closure because they elongate nearly perpendicular to the septum. Misaligned spindles, on the other hand, start elongating almost parallel to the septum plane, and thus the closing septum often confines the spindle to one daughter cell (**Figure S4**). Our results suggest that the mechanism of spindle alignment by interphase MTs is important for correct nuclear segregation in conditions where the other alignment mechanisms (cell shape and astral MTs) are impaired and may, therefore, be of evolutionary advantage.

In summary, *S. pombe* spindles attain proper alignment at two mitotic stages (beginning of mitosis and Phase III/anaphase B) by three mechanisms (driven by interphase MTs, as revealed in this study, and by cell shape and astral MTs [18]; **Figure 4**). At the very

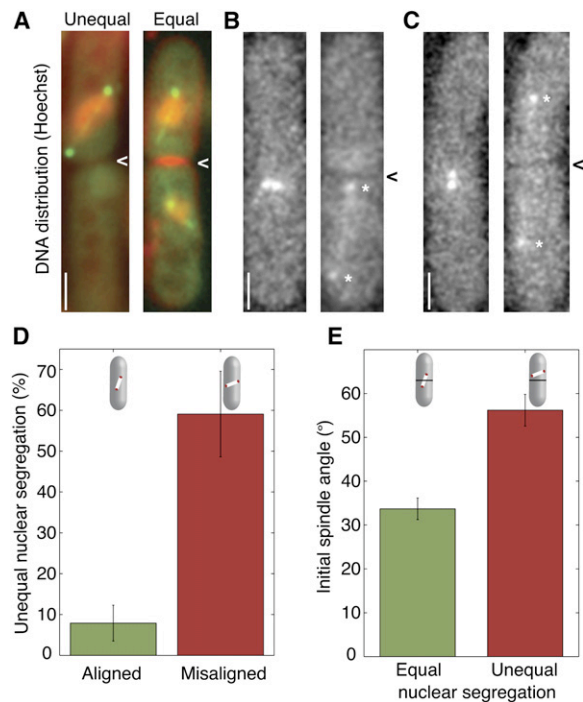


**Figure 3. Initial Misalignment of the Spindles Can Lead to Anucleate Cells when Spindle Elongation Is Slow**

(A) Inheritance of the SPBs (green dots, Sid4-GFP) correlates with the inheritance of the nuclei/chromatin (red, Hoechst staining of DNA). Left: the cells that segregated both SPBs into one daughter cell segregated the chromatin to the same daughter (unequal nuclear segregation; n = 32 out of 32 cells). Right: 90% of the cells that segregated one SPB into each daughter cell showed equal segregation of chromatin between the daughters (equal nuclear segregation; n = 48 mother cells). In the remaining 10% of the cells, nuclear segregation was unclear and/or incomplete (**Figure S4**). The arrowheads point to the septum. Scale bar in (A)–(C) represents 2 μm. (B) A cell with an initially misaligned spindle divided into one anucleate and one binucleate cell (**Movie S6**). Both SPBs (asterisks) were found in the lower daughter cell at the time when the septum formed (arrowhead). (C) A cell with an initially aligned spindle divided into two normal uninucleate cells (**Movie S7**). One SPB (asterisk) was found in each daughter cell, on the opposite side of the septum (arrowhead). (D) The cells with initially highly misaligned spindles (red, 70° < α < 90°, n = 22, mean 59.1%, 95% confidence interval for binomial data: 36.4%–79.3%) showed unequal nuclear segregation 7.5 times more frequently than the cells with well-aligned spindles (green, 0° < α < 20°, n = 38, mean 7.9%, 95% confidence interval: 1.7%–21.4%, p = 4 · 10<sup>-6</sup>). The error bars were calculated as the standard deviation of the binomial distribution (p(1 - p)/n)<sup>1/2</sup>, where p is the probability of a cell showing unequal nuclear segregation and n is the number of cells. (E) The spindles that segregated the nuclei unequally (red, n = 42) were highly significantly more misaligned at the start of mitosis than the spindles that segregated the nuclei equally (green, n = 95, p = 10<sup>-6</sup>). Error bars indicate SEM.

beginning of mitosis, the newly formed spindle is already well aligned with the cell axis. We propose that the interphase MTs attached to the duplicated SPB serve as a template for SPB separation during spindle formation (**Figures 4A–4C**). Our results suggest a novel role for interphase microtubules: in addition to determining the nuclear and, consequently, the division plane position [1–3], they also determine the initial alignment of the mitotic spindle. Proper spindle alignment, in turn,

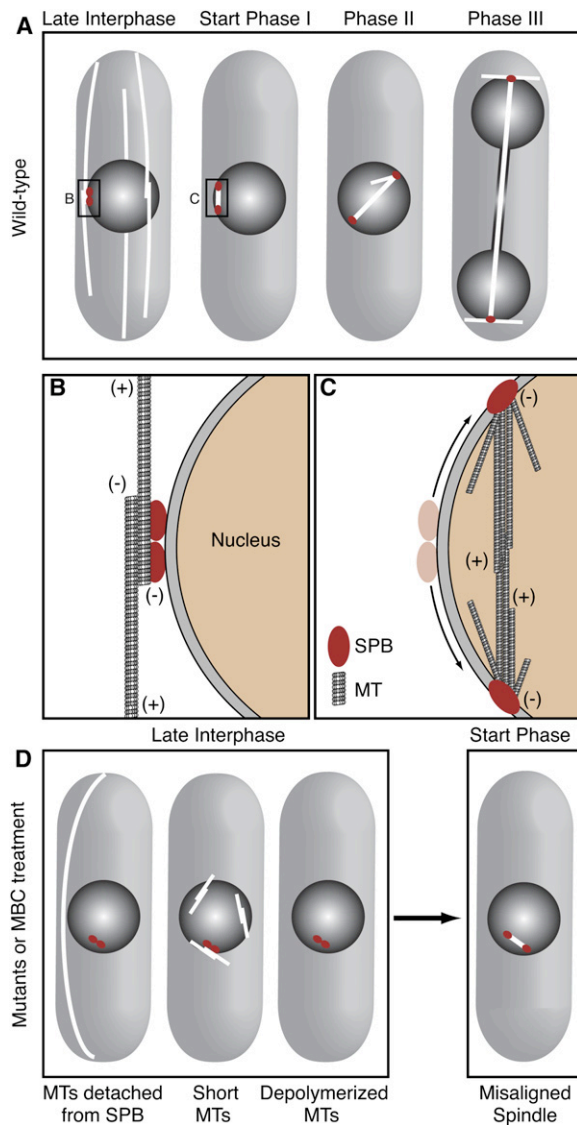


**Figure 4. A Model for Spindle Alignment in *S. pombe*:** Interphase MTs Determine the Initial Alignment, while the Cell Shape and Phase III Astral MTs Make Final Corrections

(A–C) In wild-type cells, interphase MTs align the duplicated SPB with the cell's longitudinal axis, setting the axis for future SPB separation. Consequently, the nascent spindle is well aligned with the cell axis (B and C). This alignment is lost during Phase I (prophase) and Phase II (prometaphase) through random movements of the spindle, but the loss of alignment does not delay entry into Phase III (anaphase B). Spindle alignment is corrected in Phase III, when the elongating spindle is constrained by the cell shape and assisted by pushing forces of astral MTs.

(D) Defects in interphase MT dynamics and attachment of MTs to the SPB lead to three typical phenotypes: MTs detached from the SPB (as in *mto1Δ*), short interphase MTs (as in *mal3Δ*), or no interphase MTs (as after treatment with MT-depolymerizing drugs). Since the mechanism of SPB alignment by interphase MTs is impaired in these conditions, the spindles are formed misaligned at the beginning of the subsequent mitosis.

facilitates correct segregation of chromosomes across the division plane (Figure 3). This work in fission yeast may help to clarify similar mechanisms in higher eukaryotes where spatial cues in interphase determine the

initial position of the mitotic spindle before the next cell division [24, 25].

#### Supplemental Data

Supplemental Data include four figures, seven tables, eight movies, Results, and Experimental Procedures and can be found with this article online at <http://www.current-biology.com/cgi/content/full/17/5/438/DC1/>.

#### Acknowledgments

We thank K. Gould, S. Oliferenko, J. Millar, T. Toda, D. Brunner, G. Thon, and Y. Hiraoka for yeast strains and plasmids; J. Peychl, S. Gerwig, and M. Weber from the Light Microscopy Facility at the MPI-CBG for help with the microscopes; J. Millar and S. Oliferenko for discussions; S.W. Grill, S.F. Tolic-Nørrelykke, P. Tomancak, J. Howard, A.A. Hyman, and J. Pecreaux for comments on the manuscript; and J. Nicholls for proof-reading.

Received: August 2, 2006

Revised: January 10, 2007

Accepted: January 17, 2007

Published online: February 15, 2007

#### References

1. Tolic-Norrelykke, I.M., Sacconi, L., Stringari, C., Raabe, I., and Pavone, F.S. (2005). Nuclear and division-plane positioning revealed by optical micromanipulation. *Curr. Biol.* **15**, 1212–1216.
2. Tran, P.T., Marsh, L., Doye, V., Inoue, S., and Chang, F. (2001). A mechanism for nuclear positioning in fission yeast based on microtubule pushing. *J. Cell Biol.* **153**, 397–411.
3. Daga, R.R., and Chang, F. (2005). Dynamic positioning of the fission yeast cell division plane. *Proc. Natl. Acad. Sci. USA* **102**, 8228–8232.
4. Oliferenko, S., and Balasubramanian, M.K. (2002). Astral microtubules monitor metaphase spindle alignment in fission yeast. *Nat. Cell Biol.* **4**, 816–820.
5. Gachet, Y., Tournier, S., Millar, J.B., and Hyams, J.S. (2001). A MAP kinase-dependent actin checkpoint ensures proper spindle orientation in fission yeast. *Nature* **412**, 352–355.
6. Gachet, Y., Tournier, S., Millar, J.B., and Hyams, J.S. (2004). Mechanism controlling perpendicular alignment of the spindle to the axis of cell division in fission yeast. *EMBO J.* **23**, 1289–1300.
7. Tournier, S., Gachet, Y., Buck, V., Hyams, J.S., and Millar, J.B. (2004). Disruption of astral microtubule contact with the cell cortex activates a Bub1, Bub3, and Mad3-dependent checkpoint in fission yeast. *Mol. Biol. Cell* **15**, 3345–3356.
8. Ding, R., West, R.R., Morphew, D.M., Oakley, B.R., and McIntosh, J.R. (1997). The spindle pole body of *Schizosaccharomyces pombe* enters and leaves the nuclear envelope as the cell cycle proceeds. *Mol. Biol. Cell* **8**, 1461–1479.
9. Uzawa, S., Li, F., Jin, Y., McDonald, K.L., Braunfeld, M.B., Agard, D.A., and Cande, W.Z. (2004). Spindle pole body duplication in fission yeast occurs at the G1/S boundary but maturation is blocked until exit from S by an event downstream of *cdc10+*. *Mol. Biol. Cell* **15**, 5219–5230.
10. Hagan, I.M. (1998). The fission yeast microtubule cytoskeleton. *J. Cell Sci.* **111**, 1603–1612.
11. Sawin, K.E., Lourenco, P.C., and Snaith, H.A. (2004). Microtubule nucleation at non-spindle pole body microtubule-organizing centers requires fission yeast centrosomin-related protein mod20p. *Curr. Biol.* **14**, 763–775.
12. Venkatram, S., Tasto, J.J., Feoktistova, A., Jennings, J.L., Link, A.J., and Gould, K.L. (2004). Identification and characterization of two novel proteins affecting fission yeast gamma-tubulin complex function. *Mol. Biol. Cell* **15**, 2287–2301.
13. Zimmerman, S., and Chang, F. (2005). Effects of gamma-tubulin complex proteins on microtubule nucleation and catastrophe in fission yeast. *Mol. Biol. Cell* **16**, 2719–2733.
14. Beinbauer, J.D., Hagan, I.M., Hegemann, J.H., and Fleig, U. (1997). Mal3, the fission yeast homologue of the human

- APC-interacting protein EB-1 is required for microtubule integrity and the maintenance of cell form. *J. Cell Biol.* **139**, 717–728.
15. Busch, K.E., and Brunner, D. (2004). The microtubule plus end-tracking proteins mal3p and tip1p cooperate for cell-end targeting of interphase microtubules. *Curr. Biol.* **14**, 548–559.
  16. Russell, P., and Nurse, P. (1986). *cdc25+* functions as an inducer in the mitotic control of fission yeast. *Cell* **45**, 145–153.
  17. Brunner, D., and Nurse, P. (2000). CLIP170-like tip1p spatially organizes microtubular dynamics in fission yeast. *Cell* **102**, 695–704.
  18. Tolic-Norrelykke, I.M., Sacconi, L., Thon, G., and Pavone, F.S. (2004). Positioning and elongation of the fission yeast spindle by microtubule-based pushing. *Curr. Biol.* **14**, 1181–1186.
  19. Zimmerman, S., Daga, R.R., and Chang, F. (2004). Intra-nuclear microtubules and a mitotic spindle orientation checkpoint. *Nat. Cell Biol.* **6**, 1245–1246.
  20. Rajagopalan, S., Bimbo, A., Balasubramanian, M.K., and Olfierenko, S. (2004). A potential tension-sensing mechanism that ensures timely anaphase onset upon metaphase spindle orientation. *Curr. Biol.* **14**, 69–74.
  21. Lew, D.J., and Burke, D.J. (2003). The spindle assembly and spindle position checkpoints. *Annu. Rev. Genet.* **37**, 251–282.
  22. Kusch, J., Liakopoulos, D., and Barral, Y. (2003). Spindle asymmetry: a compass for the cell. *Trends Cell Biol.* **13**, 562–569.
  23. Yeh, E., Skibbens, R.V., Cheng, J.W., Salmon, E.D., and Bloom, K. (1995). Spindle dynamics and cell cycle regulation of dynein in the budding yeast, *Saccharomyces cerevisiae*. *J. Cell Biol.* **130**, 687–700.
  24. Simons, M., and Walz, G. (2006). Polycystic kidney disease: cell division without a clue? *Kidney Int.* **70**, 854–864.
  25. Stumpff, J., Kellogg, D.R., Krohne, K.A., and Su, T.T. (2005). *Drosophila* Wee1 interacts with members of the gammaTURC and is required for proper mitotic-spindle morphogenesis and positioning. *Curr. Biol.* **15**, 1525–1534.
  26. Nabeshima, K., Nakagawa, T., Straight, A.F., Murray, A., Chikashige, Y., Yamashita, Y.M., Hiraoka, Y., and Yanagida, M. (1998). Dynamics of centromeres during metaphase-anaphase transition in fission yeast: Dis1 is implicated in force balance in metaphase bipolar spindle. *Mol. Biol. Cell* **9**, 3211–3225.